

Guiding Text-to-Image Diffusion Model Towards Grounded Generation

Ziyi Li^{1*}, Qinye Zhou^{1*}, Xiaoyun Zhang¹, Ya Zhang^{1,2}, Yanfeng Wang^{1,2}, and Weidi Xie^{1,2,†}

¹Coop. Medianet Innovation Center, Shanghai Jiao Tong University, China

²Shanghai AI Laboratory, China

https://lipurple.github.io/Grounded_Diffusion/

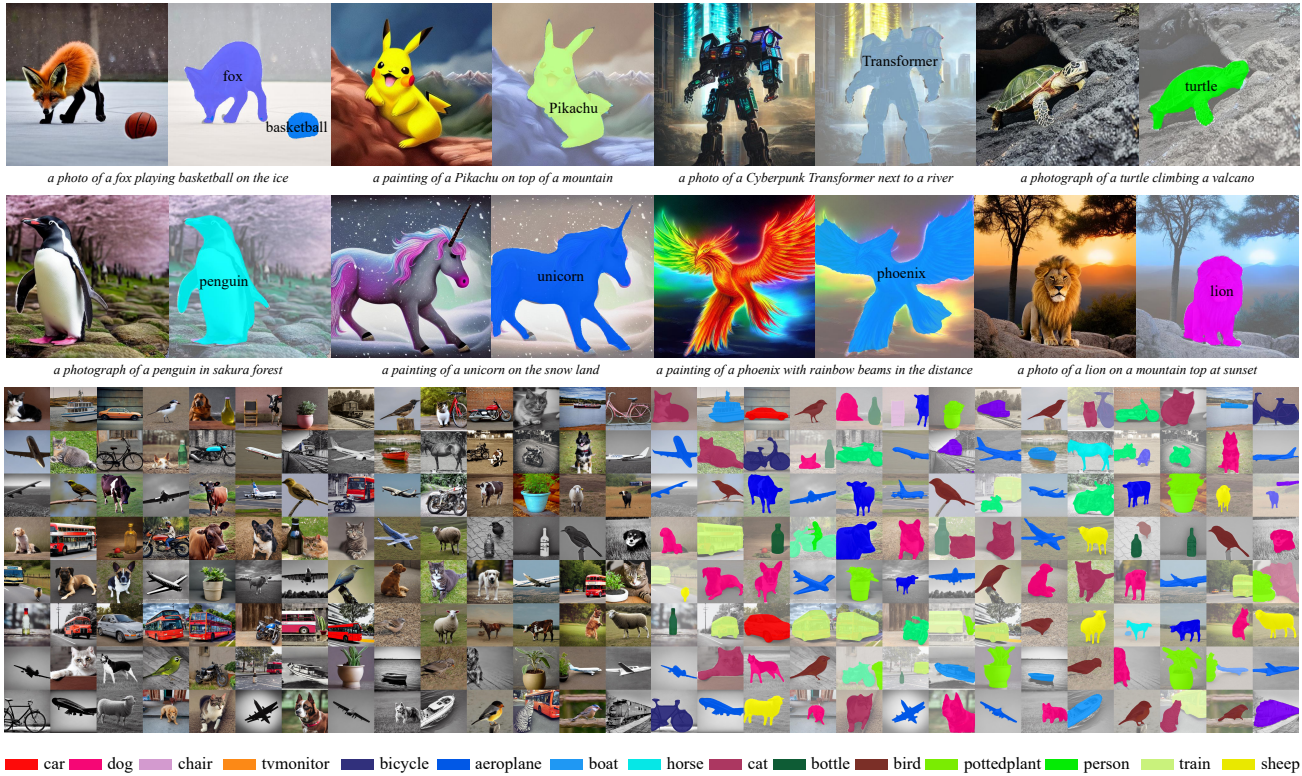


Figure 1. **Predictions from our guided text-to-image diffusion model.** The model is able to simultaneously generate images and segmentation masks for the corresponding visual objects described in the text prompt, for example, Pikachu, Unicorn, Phoenix, etc.

Abstract

The goal of this paper is to augment a pre-trained text-to-image diffusion model with the ability of open-vocabulary objects grounding, i.e., simultaneously generating images and segmentation masks for the corresponding visual entities described in the text prompt. We make the following contributions: (i) we insert a grounding module into the existing diffusion model, that can be trained to align the visual and textual embedding space of the diffusion model with only a small number of object categories; (ii) we propose an automatic pipeline for constructing a dataset, that con-

sists of $\{\text{image, segmentation mask, text prompt}\}$ triplets, to train the proposed grounding module; (iii) we evaluate the performance of open-vocabulary grounding on images generated from the text-to-image diffusion model and show that the module can well segment the objects of categories beyond seen ones at training time, as shown in Fig. 1; (iv) we adopt the guided diffusion model to build a synthetic semantic segmentation dataset, and show that, training a standard segmentation model on such dataset demonstrates competitive performance on zero-shot segmentation (ZS3) benchmark, which opens up new opportunities for adopting the powerful diffusion model for discriminative tasks.

* Both the authors have contributed equally to this project.

† denotes corresponding author.

1. Introduction

In the recent literature, text-to-image generative models have gained increasing attention from the research community and wide public, one of the main advantages of such models is the strong semantic correspondence between visual and language, learned from a large corpus of image-caption pairs, such correspondence, for instance, enables to generate photorealistic images from the free-form text prompt [26, 27, 30, 41]. While the synthesis ability of these models are unprecedented, they generally lack the ability to ground the objects within generated images, which can be crucial to a number of applications, for example, image editing, visual question answering, and visual reasoning.

In this paper, we aim to augment an existing text-to-image diffusion model with the ability of objects grounding, *i.e.*, simultaneously generating photorealistic images and segmentation masks for corresponding visual objects described in the text prompt. Generally speaking, two challenges exist: *first*, to explicitly establish the visual-language correspondence for the generative model, image-segmentation pairs are required for visual demonstrations. In previous work, for example, DatasetGAN [42] and Big-DatasetGAN [18], the authors consider collecting manual annotations for synthetic images, however, such a strategy is unlikely to be scalable, given the high annotation cost; *second*, it is unclear how to guide the generative model towards open-vocabulary grounding, *i.e.*, the model should be capable of segmenting objects from any category it can generate. In a concurrent work (DAAM [33]), attention maps are directly upsampled and aggregated at each time step to explore the influence area of each input word, despite being simple, the performance of grounding is unsatisfactory, and tends to result in ambiguities, as the text embedding for individual visual entity has been largely influenced by other entities and the global sentence at the stage of text encoding.

To tackle the challenges mentioned above, we make the following contributions: (i) we develop an automatic pipeline for automatically constructing {image, segmentation, text prompt} triplets, in particular, we adopt an off-the-shelf object detector, and do inference on images generated from the existing stable diffusion model. Theoretically, such a pipeline enables to generate infinite data samples for each of the categories within the vocabulary of existing object detector, for example, we adopt the Mask R-CNN [22] pre-trained on COCO with 80 categories; (ii) we propose a novel architecture that can segment any visual entity mentioned in the text prompt from the generated image, specifically, we propose a fusion module that explicitly aligns the visual and textual embedding space of the diffusion model, as a result, despite being only trained on a pre-defined set of object categories, the grounding module enables to segment objects of unseen ones at training time, resembling an open-vocabulary knowledge induction procedure. As shown in

Fig. 1, our guided stable diffusion model enables to segment the objects well beyond the vocabulary of any off-the-shelf detector, for example, Pikachu, unicorn, phoenix, *etc.*

To quantitatively validate the effectiveness of our proposed open-vocabulary grounding, we initiate two protocols for evaluation: *first*, we train the grounding module on the constructed training set, and compare the grounding performance with a strong off-the-shelf object detector; *second*, we adopt the guided stable diffusion model to construct a synthesized semantic segmentation dataset, and train a segmentation model on it. While evaluating on the existing benchmarks for zero-shot segmentation (ZS3), the segmentation model shows competitive performance over prior state-of-the-art models, especially on unseen categories, reflecting the effectiveness of our open-vocabulary grounding module. Crucially, it has demonstrated a promising application for applying the powerful diffusion model for discriminative tasks, that is, to expand the vocabulary beyond any existing detector can do.

2. Related Work

Image Generation. Image generation is one of the most challenging tasks in computer vision due to the high-dimensional nature of images. In the past few years, generative adversarial networks (GAN) [10], variational autoencoders (VAE) [17], flow-based models [16] and autoregressive models (ARM) [34] have made great progress. However, even GANs, the best of these methods, still face training instability and mode collapse issues [2]. Recently, Diffusion Probabilistic Models (DM) demonstrate state-of-the-art generation quality on highly diverse datasets [12, 13, 23, 29, 31], outperforming GANs in fidelity [6]. These models are often combined with a well-designed text encoder and trained on billions of image-caption pairs for text-to-image generation task, *i.e.*, OpenAI’s DALL-E 2 [26], Google’s Imagen [30] and Stability AI’s Stable Diffusion [27]. However, despite being able to generate images with impressive quality using free-form text, it remains unclear what extent the visual-language correspondence has been successfully captured, this paper aims to augment an existing text-to-image diffusion model with the ability to ground objects in its generation procedure.

Visual Grounding. Visual grounding, also known as referring expression comprehension, expects to understand the natural language query and then find out the target object of the query in an image. Early visual grounding works are trained in two stages [14, 21, 35, 36, 38], by first detecting the candidate regions, and then ranking these regions. Later, one-stage approaches [19, 28, 39, 40] attract more attention due to their superior accuracy and efficiency in fusing linguistic context and visual features. Here, we consider visual grounding in the image generation procedure.

3. Methodology

In this paper, we aim to introduce a knowledge induction procedure, that converts an existing text-to-image diffusion model for grounded generation, *i.e.*, simultaneously generating images and the segmentation mask of corresponding objects described in the text prompt. In particular, our core idea is to exploit a handful of image-segmentation pairs as visual demonstrations, to build the general visual-language correspondence between the visual representation from diffusion model and the free-form text.

In the following sections, we start by describing the problem scenario for grounded generation based on diffusion model; in Sec. 3.2, we present preliminary background knowledge of diffusion model, and terminologies that will be used in later sections; in Sec. 3.3, we detail the proposed knowledge induction procedure, including (i) the architecture design that enables to align the visual and textual embedding under an open-vocabulary setting, (ii) the training procedure based on the automatically constructed {image, segmentation, text prompt} triplets.

3.1. Problem Scenario

Assuming there exists a strong text-to-image diffusion model, for example, Stable Diffusion [27] in our case, the goal is to convert it into a grounded generation model:

$$\{\mathcal{I}, m\} = \Phi_{\text{diffusion}^+}(\epsilon, y) \quad (1)$$

where $\Phi_{\text{diffusion}^+}(\cdot)$ refers to a pre-trained text-to-image diffusion model with our grounding module appended, it takes the sampled noise ($\epsilon \sim \mathcal{N}(0, I)$) and language description y as input, and generates an image ($\mathcal{I} \in \mathbb{R}^{H \times W \times 3}$) with corresponding segmentation masks ($m \in \{0, 1\}^{H \times W \times \mathcal{O}}$) for a total of \mathcal{O} objects of interest. **Note that**, we expect the model to be *open-vocabulary*, that means, it should be able to output the corresponding segmentation mask for any objects that can be generated by diffusion model, without limitation of the semantic categories.

3.2. Preliminary on Diffusion Model

Diffusion models refer to a series of probabilistic generative models, that are trained to learn a data distribution by gradually denoising the randomly sampled Gaussian noises. Theoretically, the procedure refers to learning the reverse process of a fixed Markov Chain of length T . As for text-to-image synthesis, given a dataset of image-caption pairs, *i.e.*, $\mathcal{D}_{\text{train}} = \{(\mathcal{I}_1, y_1), \dots, (\mathcal{I}_N, y_N)\}$, the models can be interpreted as an equally weighted sequence of conditional denoising neural network that iteratively predicts a denoised variant of the input conditioned on the text prompt, $\epsilon_{\theta}(\mathcal{I}_i^t, t, y_i)$, where \mathcal{I}_i^t denotes a noisy version of the input image, and $t = 1, \dots, T$ refers to the timestep,

$i \in \{1, \dots, N\}$. For simplicity, we only describe the training and inference procedure for a single image, thus ignoring the subscript in the following sections.

In particular, this paper builds on a variant of diffusion model, namely, Stable Diffusion [27], which encodes all images with a variational autoencoder, and transfers the diffusion process to latent space. we will briefly describe its architecture and training procedure in the following.

Architecture. Stable Diffusion consists of three components: a text encoder for producing text embeddings; a pre-trained variational autoencoder (VAE) that encodes and decodes latent vectors for images; and a time-conditional UNet ($\epsilon_{\theta}(\cdot)$) for gradually denoising the latent vectors, with the progressive convolutional operation that downsamples and upsamples the visual feature maps with skip connections. The visual-language interaction occurs in the UNet, where the embeddings of the visual and textual features interact through cross-attention layers. Specifically, a text encoder is used to project the text prompt y to textual embeddings, that then are mapped into `Key` and `Value`, the spatial feature map of the noisy image is linearly projected into `Query`, and iteratively attending the conditioned text prompt for updating.

Training and Inference. The training procedure of Stable Diffusion can be described as follows: given a training pair (\mathcal{I}, y) , the input image \mathcal{I} is first mapped to a latent vector z and get a variably-noised vector $z^t := \alpha^t z + \sigma^t \epsilon$, where $\epsilon \sim \mathcal{N}(0, 1)$ is a noise term and α^t, σ^t are terms that control the noise schedule and sample quality. At training time, the time-conditional UNet is optimised to predict the noise ϵ and recover the initial z , conditioned on the text prompt y , the model is trained with a squared error loss on the predicted noise term as follows:

$$\mathcal{L}_{\text{diffusion}} = \mathbb{E}_{z, \epsilon \sim \mathcal{N}(0, 1), t, y} \left[\|\epsilon - \epsilon_{\theta}(z^t, t, y)\|_2^2 \right] \quad (2)$$

where t is uniformly sampled from $\{1, \dots, T\}$.

At inference time, Stable Diffusion is sampled by iteratively denoising $z^T \sim \mathcal{N}(0, I)$ conditioned on the text prompt y . Specifically, at each denoising step $t = 1, \dots, T$, z^{t-1} is obtained from both z^t and the predicted noise term of UNet whose input is z^t and text prompt y . After the final denoising step, z^0 will be mapped back to yield the generated image \mathcal{I} .

3.3. Open-vocabulary Grounding

In this section, our goal is to learn the correspondence between the visual representation (from the diffusion model) and category embeddings in text form, augmenting the off-the-shelf Stable Diffusion with an open-vocabulary object grounding module, as shown in Fig. 2 (left). Assuming there exists a training set of N triplets, *i.e.*, $\mathcal{D}_{\text{train}} =$

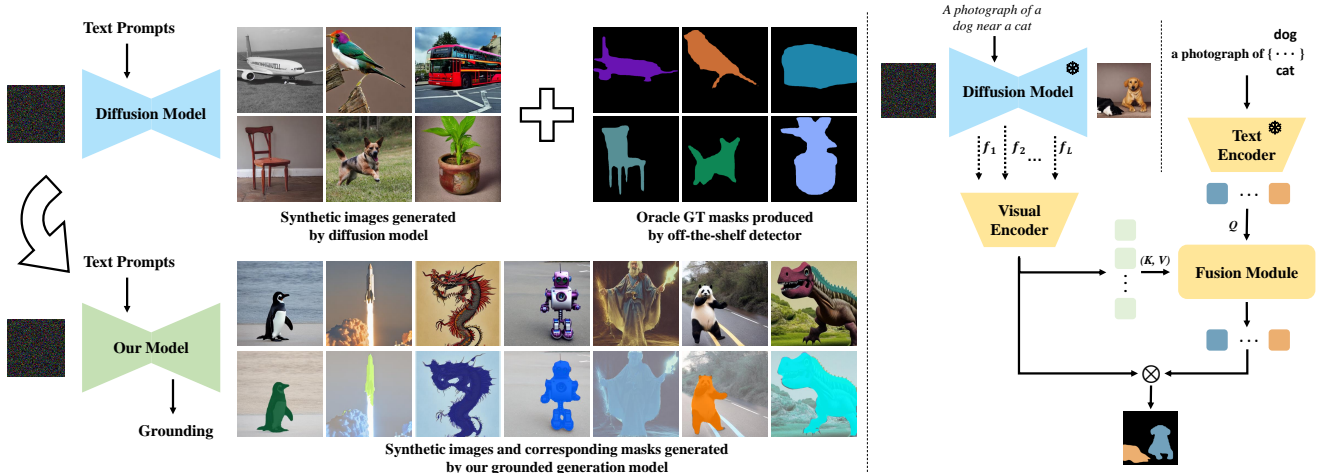


Figure 2. **Overview.** The **left** figure shows the knowledge induction procedure, where we first construct a dataset with synthetic images from diffusion model and generate corresponding oracle groundtruth masks by an off-the-shelf object detector, which is used to train the open-vocabulary grounding module. The **right** figure shows the architectural detail of our grounding module, that takes the text embeddings of corresponding entities and the visual features extracted from diffusion model as input, and outputs the corresponding segmentation masks. During training, both the diffusion model and text encoders are kept *frozen*.

$\{(\mathcal{F}_1, m_1^{\text{gt}}, y_1), \dots, (\mathcal{F}_N, m_N^{\text{gt}}, y_N)\}$, the predicted segmentation mask for all objects, *i.e.*, $m_i \in \mathbb{R}^{H \times W \times \mathcal{O}_i}$ can be obtained by:

$$m_i = \Phi_{\text{fuse}}(\Phi_{\text{v-enc}}(f_i^1, \dots, f_i^n), \Phi_{\text{t-enc}}(g(y_i))) \quad (3)$$

where y_i denotes the text prompt for image generation, $\mathcal{F}_i = \{f_i^1, \dots, f_i^n\}$ refers to the intermediate representation from Stable Diffusion at $t = 5$ (this has been experimentally validated in Sec. 4.3), $\Phi_{\text{v-enc}}(\cdot)$, $\Phi_{\text{t-enc}}(\cdot)$ and $\Phi_{\text{fuse}}(\cdot)$ denote the visual encoder, text encoder, and fusion module. At training time, $g(\cdot)$ denotes a group of templates that decorates each of the visual categories in the text prompt, *e.g.*, ‘a photograph of a [category name]’. There are totally \mathcal{O}_i object categories in the text prompt, and they fall into a pre-defined set of vocabularies $\mathcal{C}_{\text{train}}$. **It is important to mention that**, we expect the visual-language correspondence to be highly generalizable, such that the grounding module should equally be capable of segmenting objects from unseen categories at test time, *i.e.*, $\mathcal{C}_{\text{test}} \supset \mathcal{C}_{\text{train}}$.

In the following sections, we start by introducing the procedure for automatically constructing the training set in Sec. 3.3.1, followed by the architecture design for open-vocabulary grounding in Sec. 3.3.2, lastly, we detail the training process via knowledge induction in Sec. 3.3.3.

3.3.1. Dataset Construction

Here, we introduce the idea to construct the training set with {visual feature, segmentation, text prompt} triplets, specifically, we develop an automatic pipeline to construct the {image, segmentation, text prompt} triplets, thus the visual feature can be obtained from Stable Diffusion via the forward inference to generate the image.

In practise, we prepare a vocabulary with common object categories, for example, the classes in PASCAL VOC can form a category set as $\mathcal{C}_{\text{pascal}} = \{\text{‘dog’}, \text{‘cat’}, \dots\}$, $|\mathcal{C}_{\text{pascal}}| = 20$, we randomly select a number of classes to construct a text prompt for image generation (*e.g.*, ‘a photograph of a dog and cat’). Repeating the above operation, we can theoretically generate infinite amount of image and text prompt pairs. To acquire the segmentation masks, we take an off-the-shelf object detector, *e.g.*, pre-trained Mask R-CNN [22], and run the inference procedure on the generated images:

$$m_i^{\text{gt}} = \Phi_{\text{detector}}(\mathcal{I}_i), \quad \text{where } \mathcal{I}_i = \Phi_{\text{diffusion}}(\epsilon, y_i), \quad (4)$$

where $m_i^{\text{gt}} \in \{0, 1\}^{H \times W \times \mathcal{O}_i}$ refers to the predicted masks for a total of \mathcal{O}_i objects in the generated image \mathcal{I}_i , conditioning on the text prompt y_i .

To evaluate the effectiveness of the induction procedure for open-vocabulary grounding, we divide the vocabulary set into seen categories ($\mathcal{C}_{\text{seen}}$) and unseen categories ($\mathcal{C}_{\text{unseen}}$), the training set ($\mathcal{D}_{\text{train}}$) only has images of seen categories, and the test set ($\mathcal{D}_{\text{test}}$) has both seen and unseen categories.

3.3.2. Architecture

Given one specific training triplet $(\mathcal{F}_i, m_i^{\text{gt}}, y_i)$, we now detail three trainable components in the proposed grounding module: visual encoder, text encoder, and fusion module.

Visual Encoder. Given the visual representation from Stable Diffusion, we concatenate features with the same spatial resolution (from UNet encoding and decoding path) to obtain $\{f_i^1, \dots, f_i^n\}$, where $f_i^k \in \mathbb{R}^{\frac{h}{2^k} \times \frac{w}{2^k} \times d_k}$, $k \in$

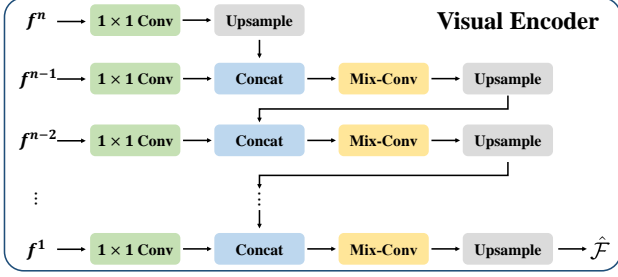


Figure 3. **The architecture of visual encoder.** The features extracted from UNet are first grouped according to their resolution, then gradually upsampled and fused into the final visual feature.

$\{0, \dots, n\}$ denotes layer indices of UNet, d_k refers to the feature dimension.

Next, we input $\{f_i^1, \dots, f_i^n\}$ to visual encoder for generating the fused visual feature $\hat{\mathcal{F}}_i = \Phi_{v\text{-enc}}(\{f_i^1, \dots, f_i^n\})$. As shown in Fig 3, visual encoder consists of 4 types of blocks: (1) 1×1 Conv for reducing feature dimensionality, (2) Upsample for upsampling the feature to a higher spatial resolution, (3) Concat for concatenating features, and (4) Mix-conv for blending features from different spatial resolutions, that includes two 3×3 Conv operations with residual connection and a conditional batchnorm operation, similar to [18].

Text Encoder. We adopt the language model from pre-trained Stable Diffusion, specifically, given the text prompt y_i , the text encoder output the corresponding embeddings for all visual objects: $\mathcal{E}_{\text{obj}_i} = \Phi_{t\text{-enc}}(g(y_i))$.

Fusion Module. The fusion module computes interaction between visual features and text embeddings, then outputs segmentation masks for all visual objects. In specific, we use a standard transformer decoder with three layers, the text embeddings are treated as Query, that iteratively attend the visual feature for updating, and are further converted into per-segmentation embeddings with a Multi-Layer Perceptron (MLP). The object segmentation masks can be obtained by dot product visual features with the per-segmentation embeddings. Formally, the procedure can be denoted as :

$$\mathcal{E}_{\text{seg}_i} = \Phi_{\text{TRANSFORMER-D}}(W^Q \cdot \mathcal{E}_{\text{obj}_i}, W^K \cdot \hat{\mathcal{F}}_i, W^V \cdot \hat{\mathcal{F}}_i) \quad (5)$$

$$m_i = \hat{\mathcal{F}}_i \cdot [\Phi_{\text{MLP}}(\mathcal{E}_{\text{seg}_i})]^T \quad (6)$$

where the transformer decoder generates per-segmentation embedding $\mathcal{E}_{\text{seg}_i} \in \mathbb{R}^{N \times d_e}$ for all visual objects described in the text prompt, W^Q, W^K, W^V refer to the learnable parameters for Query, Key and Value projection.

3.3.3. Training

With the constructed dataset, we can now start supervised training the proposed grounding module:

$$\mathcal{L} = -\frac{1}{N} \sum_{i=1}^N [m_i^{\text{gt}} \cdot \log(\sigma(m_i)) + (1 - m_i^{\text{gt}}) \cdot \log(\sigma(1 - m_i))] \quad (7)$$

where $m_i^{\text{gt}} \in \mathbb{R}^{H \times W \times \mathcal{O}_i}$ refers to the oracle groundtruth segmentation from the off-the-shelf object detector, and $m_i \in \mathbb{R}^{H \times W \times \mathcal{O}_i}$ refers to the predicted segmentation from our grounding module, $\sigma(\cdot)$ refers to Sigmoid function.

In practise, while using the off-the-shelf detector to generate segmentation masks, the model may sometimes fail to detect the objects mentioned in the text prompt, and output incorrect segmentation masks. Such error comes from two sources, (i) the diffusion model may fail to generate high-quality images; (ii) off-the-shelf detector may fail to detect the objects in the synthetic image, due to the domain gap between synthetic and real images. Here, we consider two training strategies, **Normal Training**, where we fully trust the off-the-shelf detector, and use all predicted segmentation masks to train the grounding module; alternatively, we also try **Training w.o. Zero Masks**, as we empirically found that the majority of failure cases come from false negatives, that is to say, the detector failed to detect the objects and output an all-zero mask, therefore, we can train the grounding modules by ignoring the all-zero masks.

4. Experiments

In this section, we detail the evaluation detail for validating the effectiveness of objects grounding during image generation, specifically, we consider two protocols: in Sec. 4.1, we train the grounding module with the constructed training set, and test the segmentation performance on generated images from Stable Diffusion, with the detector’s output as oracle groundtruth for evaluation; in Sec. 4.2, we use the guided diffusion model to construct a synthesized semantic segmentation dataset, and train a segmentation model on it, we evaluate the model on the existing benchmarks for zero-shot segmentation. Lastly, in Sec. 4.3, we conduct a series of ablation studies on the different training strategies.

4.1. Protocol-I: Grounded Generation

Here, we train the grounding module with our constructed training set, as described in Sec. 3.3.1, specifically, the training set only consists of a subset of common (seen) categories, while the testing set consists of both seen and unseen categories. In the following, we describe the implementation and experimental results in detail, to thoroughly assess the model for grounded generation.

Following the split rule in [7, 11, 37], we adopt two different sets of categories: (i) we adopt the categories defined in PASCAL VOC [9], divide them into 15 seen categories and 5 unseen categories; (ii) we adopt the category definition in MS-COCO [20], divide them into 65 seen categories and 15 unseen categories. The dataset constructed for these two sets are called **PASCAL-sim** and **COCO-sim**, respectively.

Test Setting	# Objects	PASCAL-sim					COCO-sim				
		One		Two			One		Two		
		Categories	Seen	Unseen	Seen	Seen +Unseen	Unseen	Seen	Unseen	Seen	Seen +Unseen
DAAM [33]	Split1	61.66	75.63	46.74	51.31	69.94	62.25	55.56	49.68	52.06	43.35
	Split2	65.75	59.25	49.08	47.98	41.50	60.08	65.55	48.80	54.66	33.22
	Split3	67.11	53.82	48.80	48.28	41.41	62.81	52.48	50.85	49.84	45.80
	Average	64.84	62.90	48.21	49.19	50.95	61.71	57.76	49.78	52.19	40.79
Ours	Split1	90.16	83.19	78.93	66.07	57.93	83.35	76.81	64.64	57.15	47.77
	Split2	90.08	86.19	78.68	67.10	47.21	82.83	74.93	63.39	57.18	42.82
	Split3	90.67	79.86	79.68	70.42	62.07	84.85	67.89	65.70	54.60	42.62
	Average	90.30	83.08	79.10	67.86	55.74	83.68	73.21	64.16	56.31	44.40

Table 1. **Quantitative result for Protocol-I evaluation on grounded generation.** Our model has been trained on the synthesized training dataset, that consists of images with one or two objects from only seen categories, and test on our synthesized test dataset that consists of images with one or two objects of both seen and unseen categories. Split1, Split2 and Split3 refer to 3 different splits of \mathcal{C} that construct 3 different $(\mathcal{C}_{\text{seen}}, \mathcal{C}_{\text{unseen}})$ pairs, respectively. Our model outperforms the DAAM [33], by a large margin, see text for more detailed discussion.

Training Set. For PASCAL-sim or COCO-sim, we generate a synthetic training set by randomly sampling images from pre-trained Stable Diffusion. This exposes our grounding module to a great variety of data ($> 40k$) at training time, and the model is unlikely to see the same labeled examples twice during training. In contrast to previous work, such as BigDatesetGAN [18], where only a single object is considered, we construct the text prompt with one or two objects at a time, note that, for training, only the seen categories are sampled. Although we can certainly generate images with more than two object categories, the quality of the generated images tends to be unstable, limited by the generation ability of Stable Diffusion, thus we only consider synthesized images with less than three object categories.

Testing Set. For the evaluation purpose, we generate two synthetic test sets with offline sampling for PASCAL-sim and COCO-sim, respectively. In total, we have collected about 1k images for PASCAL-sim, and about 5k images for COCO-sim, we run the off-the-shelf object detector on these generated images to produce the oracle groundtruth segmentation. For both test sets, the images containing two categories will be divided into three groups: both seen, both unseen, one seen and one unseen. We leave the detailed statistics of our synthetic dataset in the supplementary material. **Note that**, we have manually checked all the images and the oracle groundtruth segmentation produced from the off-the-shelf detector, and only keep the high-quality ones, thus the performance evaluation of the grounding module can be a close proxy.

Evaluation Metrics. We use the category-wise mean intersection-over-union (mIoU) as evaluation metric, defined as averages of IoU over all the categories: $\text{mIoU} = \frac{1}{C} \sum_{c=1}^C \text{IoU}_c$, where C is the number of all target categories, and IoU_c is the intersection-over-union for the category with index is c .

Implementation Details. We use the pre-trained Stable

Diffusion [27] and the text encoder of CLIP [25] in our implementation. We choose the Mask R-CNN [22] trained on COCO dataset as our object detector for oracle groundtruth segmentation. We fuse features from U-Net and upsample them into 512×512 spatial resolution, the text and visual embeddings are both mapped into 512 dimension before feeding into the fusion module. We train our grounding module with two NVIDIA GeForce RTX 3090 GPUs for 5k iterations with batch size equal to 8, ADAM [15] optimiser with $\beta_1 = 0.9$, $\beta_2 = 0.999$. The initial learning rate is set to $1e-4$ and the weight decay is $1e-4$.

Results. As shown in Tab. 1, we provide experimental results for our grounded generation model, we change the composition of categories three times and compute the results for each split. Here, we can make the following observations: *first*, our model significantly outperforms the unsupervised method DAAM [33] in the mIoU on all test settings. This is because DAAM tends to result in ambiguous segmentations, as the textual embedding for individual visual entity will largely be influenced by other ones within the global sentence at the text encoding stage; *second*, our grounding module achieves superior performance on both seen and unseen categories, indicating its open-vocabulary nature, *i.e.*, the guided diffusion model can synthesize images and their corresponding segmentations for more categories beyond the vocabulary of the off-the-shelf detector, as described in Sec. 3.3.3.

Visualization. We demonstrate the visualization results in Fig. 4. On both seen and unseen categories, our model can successfully ground the objects in terms of segmentation mask. Impressively, as shown in Fig. 1, our grounding module can even segment the objects beyond any off-the-shelf detector can do, showing the strong open-vocabulary grounded generation ability of our model.

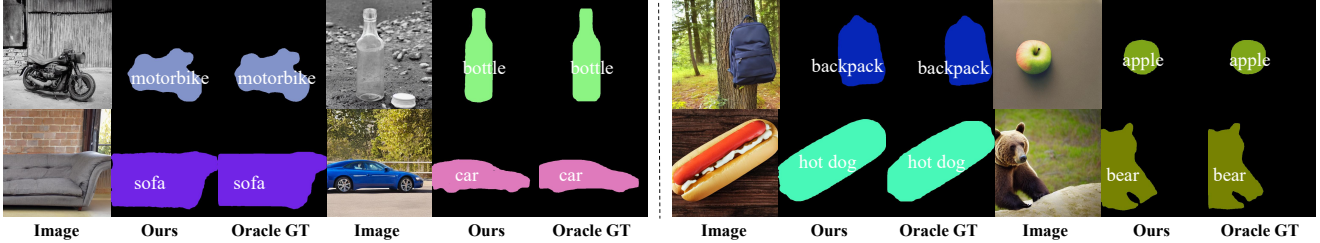


Figure 4. **Segmentation results of PASCAL-sim (left) and COCO-sim (right)** on seen (motorbike, bottle, backpack and apple) and unseen (sofa, car, hot dog and bear) categories. Our grounded generation model achieves comparable segmentation results to the oracle groundtruth generated by the off-the-shelf object detector.



Figure 5. **Our synthesized semantic segmentation dataset** with one category (left) and two categories (right) for Protocol-II training.

4.2. Protocol-II: Open-vocabulary Segmentation

In the previous protocol, we have validated the ability for open-vocabulary grounded generation, however, even after being manually checked, the oracle groundtruth from off-the-shelf detector may also be inaccurate at the boundary. Here, we introduce another experiment to validate the effectiveness of the grounding module, in particular, we first construct a synthesized image-segmentation dataset with the guided Stable Diffusion, then train a semantic segmentation model on such a synthetic dataset, and evaluate it on public image segmentation benchmarks.

Overall, the segmentation model is challenged from the following two perspectives: *first*, it has only been trained on synthetic images, that resembles a zero-shot Sim2Real transfer; *second*, the groundtruth masks for unseen object categories are generated from our guided Stable Diffusion that has only been trained on seen categories. Therefore, with such an evaluation protocol, on the one hand, it can reflect the effectiveness of our grounding module from the performance on segmenting unseen categories, and more importantly, it introduces a promising application, *i.e.*, use our guided Stable Diffusion to expand the vocabulary beyond any existing detector can do.

Dataset. In order to train the semantic segmentation model, we synthesize a dataset with 10k image-segmentation pairs for 20 categories (both seen and unseen) as shown in Fig. 5. All the image-segmentation pairs are generated by our guided Stable Diffusion, trained with only 15 seen categories in PASCAL VOC. We **do not** finetune on PASCAL

Methods	Training Dataset			mIoU		
	Type	Categories	Objects	Seen	Unseen	Harmonic
ZS3 [3]	real	15	-	78.0	21.2	33.3
SPNet [37]	real	15	-	77.8	25.8	38.8
CaGNet [11]	real	15	-	78.6	30.3	43.7
Joint [1]	real	15	-	77.7	32.5	45.9
STRICT [24]	real	15	-	82.7	35.6	49.8
SIGN [5]	real	15	-	<u>83.5</u>	41.3	55.3
ZegFormer [7]	real	15	-	86.4	63.6	73.3
Ours	synthetic	15 + 5	one	62.8	50.0	55.7
	synthetic	15 + 5	two	65.8	60.1	62.8
	synthetic	15 + 5	mixture	69.5	<u>63.2</u>	<u>66.2</u>

Table 2. **Comparison with the previous ZS3 methods on PASCAL VOC.** The “Seen”, “Unseen”, and “Harmonic” denote mIoU of seen categories, unseen categories, and their harmonic mean. These ZS3 methods are trained on PASCAL VOC training set.

VOC and only evaluate on its test set (1,449 images).

Training Details. To compare with other open-vocabulary methods, our semantic segmentation model uses MaskFormer [4] with ResNet101 as its backbone. The image resolution for training is 224×224 pix, and we train the model on our synthetic dataset for 40k iterations with batch size equal to 8. We use the ADAMW as our optimizer with a learning rate of $1e-4$ and the weight decay is $1e-4$.

Comparison on Zero-Shot Segmentation (ZS3). In Tab. 2, we compare with the existing zero-shot semantic segmentation approaches. Despite being only trained on a synthetic dataset, our model outperforms most of ZS3 approaches on unseen categories. Specifically, the model

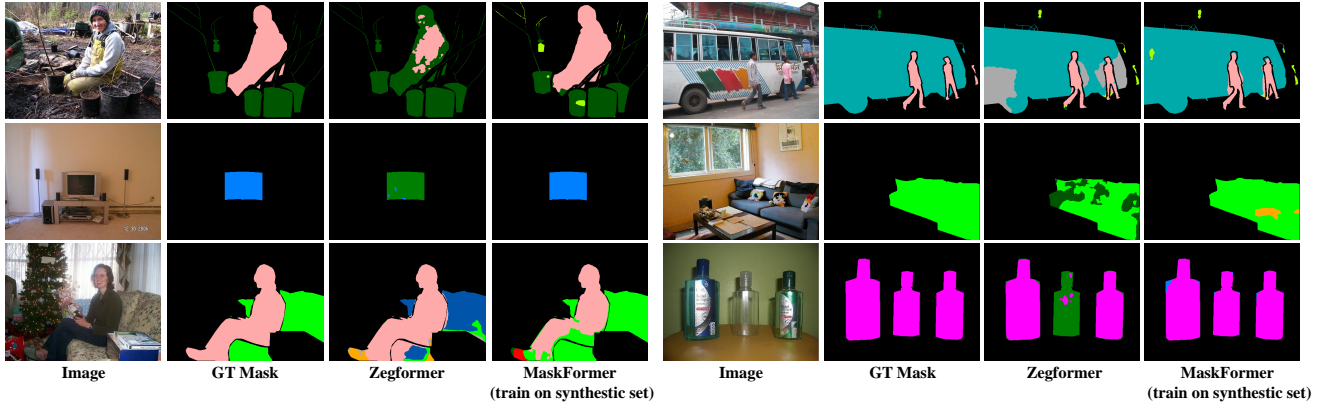


Figure 6. **Visualization of zero-shot segmentation results on Pascal-VOC.** MaskFormer trained on our synthetic dataset achieves comparable performance with Zegformer (the state-of-the-art zero-shot semantic segmentation method) in segmenting unseen categories, *i.e.* pottedplant, sofa and tvmonitor. **Note that** although MaskFormer has seen these categories during training, the image-segmentation pairs of these categories are generated with our grounding module.

Training Type	One		Two		
	Seen	Unseen	Seen	Seen +Unseen	Unseen
Normal Training	89.88	71.18	77.66	57.24	44.22
Training w.o. Zero Masks	90.16	83.19	78.93	66.07	57.93

Table 3. **Ablation on training type on the constructed dataset.** Performance is measured by mIoU on PASCAL-sim test set.

trained on the mixture of one and two objects achieves the best performance. As shown in Fig. 6, our model obtains accurate segmentation on both seen and unseen categories. Therefore, we can have the following observations: (i) the grounding module is capable of segmenting unseen categories despite it has never seen any segmentation mask during the knowledge induction procedure, validating the strong generalisation of the grounding module in the guided Stable Diffusion; (ii) it is possible to segment more object categories by simply training on synthesized datasets.

4.3. Ablation study

In this section, we show the effect of different training loss and different timestep for extracting visual representation, due to the space limitation, we refer the reader for supplementary material, for the study on the different number of objects in the synthetic datasets or seen categories, and the effect of different datasets.

Normal Training v.s. Training without Zero Masks. As shown in Tab. 3, **Normal Training** results in unsatisfactory performance on unseen categories, we conjecture this is because the errors from detector tend to be false negative, that bias our grounding module to generate all-zero segmentation masks when encountering unseen categories; in contrast, by ignoring all-zero masks at training, **Training w.o. Zero Masks** achieves equally good performance on both seen and unseen categories.

Timesteps for Extracting Visual Representation. We

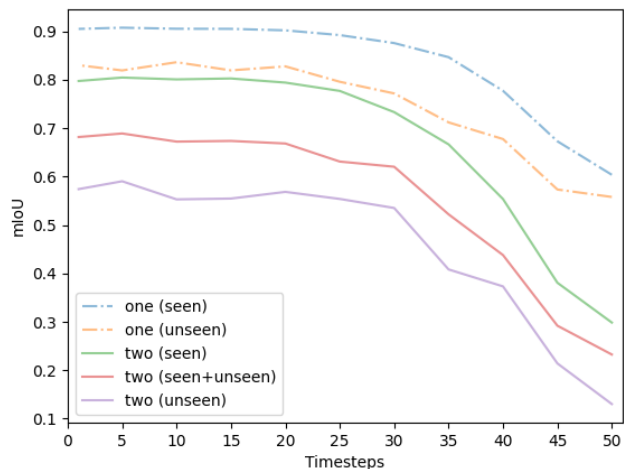


Figure 7. **Ablation on timesteps.** The mIoU is measured for the model with extracting features from Stable Diffusion in different timesteps on PASCAL-sim.

compare the performance by extracting visual representation from Stable Diffusion at different timesteps, the results on PASCAL-sim can be seen in Fig. 7, showing that as the denoising steps gradually decrease, *i.e.*, from $t = 0 \rightarrow 50$, the performance for grounding tends to decrease in general, when $t = 5$, the best result is obtained.

5. Conclusion

In this paper, we propose a novel idea for guiding the existing Stable Diffusion towards open-vocabulary grounded generation, *i.e.*, segmenting the visual entities described in the text prompt while generating images. Specifically, we introduce a grounding module that explicitly aligns the visual and textual embedding space of the Stable Diffusion and train such module with an automatically constructed dataset, consisting of {image, segmentation, text prompts} triplets. Experimentally, we show that visual-language cor-

respondence can be established by only training on a limited number of object categories, while getting the ability for open-vocabulary grounding at the image generation procedure. Additionally, we generate a synthetic semantic segmentation dataset using our guided Stable Diffusion and train a semantic segmentation model. Without finetuning, the model can directly transfer to real images, and show competitive performance to existing zero-shot semantic segmentation approaches on PASCAL VOC dataset, opening up new opportunities to exploit generative model for discriminative tasks.

References

- [1] Donghyeon Baek, Youngmin Oh, and Bumsub Ham. Exploiting a joint embedding space for generalized zero-shot semantic segmentation. In *Proc. ICCV*, 2021. 7
- [2] Andrew Brock, Jeff Donahue, and Karen Simonyan. Large scale gan training for high fidelity natural image synthesis. *arXiv preprint arXiv:1809.11096*, 2018. 2
- [3] Maxime Bucher, Tuan-Hung Vu, Matthieu Cord, and Patrick Pérez. Zero-shot semantic segmentation. *NeurIPS*, 2019. 7
- [4] Bowen Cheng, Alex Schwing, and Alexander Kirillov. Per-pixel classification is not all you need for semantic segmentation. *NeurIPS*, 2021. 7, 18
- [5] Jiaxin Cheng, Soumyaroop Nandi, Prem Natarajan, and Wael Abd-Almageed. Sign: Spatial-information incorporated generative network for generalized zero-shot semantic segmentation. In *Proc. ICCV*, 2021. 7
- [6] Prafulla Dhariwal and Alexander Nichol. Diffusion models beat gans on image synthesis. *NeurIPS*, 2021. 2
- [7] Jian Ding, Nan Xue, Gui-Song Xia, and Dengxin Dai. Decoupling zero-shot semantic segmentation. In *Proc. CVPR*, 2022. 5, 7
- [8] Alexey Dosovitskiy, Lucas Beyer, Alexander Kolesnikov, Dirk Weissenborn, Xiaohua Zhai, Thomas Unterthiner, Mostafa Dehghani, Matthias Minderer, Georg Heigold, Sylvain Gelly, et al. An image is worth 16x16 words: Transformers for image recognition at scale. *arXiv preprint arXiv:2010.11929*, 2020. 12
- [9] Mark Everingham, Luc Van Gool, Christopher KI Williams, John Winn, and Andrew Zisserman. The pascal visual object classes (voc) challenge. *International journal of computer vision(IJCV)*, 2010. 5, 14, 15, 18
- [10] Ian Goodfellow, Jean Pouget-Abadie, Mehdi Mirza, Bing Xu, David Warde-Farley, Sherjil Ozair, Aaron Courville, and Yoshua Bengio. Generative adversarial networks. *Communications of the ACM*, 2020. 2
- [11] Zhangxuan Gu, Siyuan Zhou, Li Niu, Zihan Zhao, and Liqing Zhang. Context-aware feature generation for zero-shot semantic segmentation. In *ACM MM*, 2020. 5, 7
- [12] Jonathan Ho, Ajay Jain, and Pieter Abbeel. Denoising diffusion probabilistic models. *NeurIPS*, 2020. 2
- [13] Jonathan Ho, Chitwan Saharia, William Chan, David J Fleet, Mohammad Norouzi, and Tim Salimans. Cascaded diffusion models for high fidelity image generation. *J. Mach. Learn. Res.*, 2022. 2
- [14] Richang Hong, Daqing Liu, Xiaoyu Mo, Xiangnan He, and Hanwang Zhang. Learning to compose and reason with language tree structures for visual grounding. *IEEE transactions on pattern analysis and machine intelligence(TPAMI)*, 2019. 2
- [15] Diederik P Kingma and Jimmy Ba. Adam: A method for stochastic optimization. *arXiv preprint arXiv:1412.6980*, 2014. 6
- [16] Durk P Kingma and Prafulla Dhariwal. Glow: Generative flow with invertible 1x1 convolutions. *NeurIPS*, 2018. 2
- [17] Diederik P Kingma and Max Welling. Auto-encoding variational bayes. *arXiv preprint arXiv:1312.6114*, 2013. 2
- [18] Daiqing Li, Huan Ling, Seung Wook Kim, Karsten Kreis, Sanja Fidler, and Antonio Torralba. Bigdatasetgan: Synthesizing imagenet with pixel-wise annotations. In *Proc. CVPR*, 2022. 2, 5, 6
- [19] Yue Liao, Si Liu, Guanbin Li, Fei Wang, Yanjie Chen, Chen Qian, and Bo Li. A real-time cross-modality correlation filtering method for referring expression comprehension. In *Proc. CVPR*, 2020. 2
- [20] Tsung-Yi Lin, Michael Maire, Serge Belongie, James Hays, Pietro Perona, Deva Ramanan, Piotr Dollár, and C Lawrence Zitnick. Microsoft coco: Common objects in context. In *Proc. ECCV*, 2014. 5, 14
- [21] Daqing Liu, Hanwang Zhang, Feng Wu, and Zheng-Jun Zha. Learning to assemble neural module tree networks for visual grounding. In *Proc. ICCV*, 2019. 2
- [22] Ze Liu, Yutong Lin, Yue Cao, Han Hu, Yixuan Wei, Zheng Zhang, Stephen Lin, and Baining Guo. Swin transformer: Hierarchical vision transformer using shifted windows. In *Proc. ICCV*, 2021. 2, 4, 6
- [23] Alexander Quinn Nichol and Prafulla Dhariwal. Improved denoising diffusion probabilistic models. In *ICML*, 2021. 2
- [24] Giuseppe Pastore, Fabio Cermelli, Yongqin Xian, Massimiliano Mancini, Zeynep Akata, and Barbara Caputo. A closer look at self-training for zero-label semantic segmentation. In *Proc. CVPRW*, 2021. 7
- [25] Alec Radford, Jong Wook Kim, Chris Hallacy, Aditya Ramesh, Gabriel Goh, Sandhini Agarwal, Girish Sastry, Amanda Askell, Pamela Mishkin, Jack Clark, et al. Learning transferable visual models from natural language supervision. In *ICML*, 2021. 6, 12
- [26] Aditya Ramesh, Prafulla Dhariwal, Alex Nichol, Casey Chu, and Mark Chen. Hierarchical text-conditional image generation with clip latents. *arXiv preprint arXiv:2204.06125*, 2022. 2, 16
- [27] Robin Rombach, Andreas Blattmann, Dominik Lorenz, Patrick Esser, and Björn Ommer. High-resolution image synthesis with latent diffusion models. In *Proc. CVPR*, 2022. 2, 3, 6, 12, 14, 18
- [28] Arka Sadhu, Kan Chen, and Ram Nevatia. Zero-shot grounding of objects from natural language queries. In *Proc. ICCV*, 2019. 2
- [29] Chitwan Saharia, William Chan, Huiwen Chang, Chris Lee, Jonathan Ho, Tim Salimans, David Fleet, and Mohammad Norouzi. Palette: Image-to-image diffusion models. In *ACM SIGGRAPH*, 2022. 2

- [30] Chitwan Saharia, William Chan, Saurabh Saxena, Lala Li, Jay Whang, Emily Denton, Seyed Kamyar Seyed Ghasemipour, Burcu Karagol Ayan, S Sara Mahdavi, Rapha Gontijo Lopes, et al. Photorealistic text-to-image diffusion models with deep language understanding. *arXiv preprint arXiv:2205.11487*, 2022. 2
- [31] Chitwan Saharia, Jonathan Ho, William Chan, Tim Salimans, David J Fleet, and Mohammad Norouzi. Image super-resolution via iterative refinement. *IEEE transactions on pattern analysis and machine intelligence (TPAMI)*, 2022. 2
- [32] Jiaming Song, Chenlin Meng, and Stefano Ermon. Denoising diffusion implicit models. *arXiv preprint arXiv:2010.02502*, 2020. 16
- [33] Raphael Tang, Akshat Pandey, Zhiying Jiang, Gefei Yang, Karun Kumar, Jimmy Lin, and Ferhan Ture. What the daam: Interpreting stable diffusion using cross attention. *arXiv preprint arXiv:2210.04885*, 2022. 2, 6
- [34] Aaron Van den Oord, Nal Kalchbrenner, Lasse Espeholt, Oriol Vinyals, Alex Graves, et al. Conditional image generation with pixelcnn decoders. *NeurIPS*, 2016. 2
- [35] Liwei Wang, Yin Li, Jing Huang, and Svetlana Lazebnik. Learning two-branch neural networks for image-text matching tasks. *IEEE Transactions on Pattern Analysis and Machine Intelligence (TPAMI)*, 2018. 2
- [36] Peng Wang, Qi Wu, Jiewei Cao, Chunhua Shen, Lianli Gao, and Anton van den Hengel. Neighbourhood watch: Referring expression comprehension via language-guided graph attention networks. In *Proc. CVPR*, 2019. 2
- [37] Yongqin Xian, Subhabrata Choudhury, Yang He, Bernt Schiele, and Zeynep Akata. Semantic projection network for zero-and few-label semantic segmentation. In *Proc. CVPR*, 2019. 5, 7
- [38] Sibe Yang, Guanbin Li, and Yizhou Yu. Dynamic graph attention for referring expression comprehension. In *Proc. ICCV*, 2019. 2
- [39] Zhengyuan Yang, Tianlang Chen, Liwei Wang, and Jiebo Luo. Improving one-stage visual grounding by recursive subquery construction. In *Proc. ECCV*, 2020. 2
- [40] Zhengyuan Yang, Boqing Gong, Liwei Wang, Wenbing Huang, Dong Yu, and Jiebo Luo. A fast and accurate one-stage approach to visual grounding. In *Proc. ICCV*, 2019. 2
- [41] Jiahui Yu, Yuanzhong Xu, Jing Yu Koh, Thang Luong, Gungjan Baid, Zirui Wang, Vijay Vasudevan, Alexander Ku, Yinfei Yang, Burcu Karagol Ayan, et al. Scaling autoregressive models for content-rich text-to-image generation. *arXiv preprint arXiv:2206.10789*, 2022. 2
- [42] Yuxuan Zhang, Huan Ling, Jun Gao, Kangxue Yin, Jean-Francois Lafleche, Adela Barriuso, Antonio Torralba, and Sanja Fidler. Datasetgan: Efficient labeled data factory with minimal human effort. In *Proc. CVPR*, 2021. 2

Supplementary

A Details on the Architecture of Grounding module	12
B Details on the Synthetic Dataset	13
B.1. Dataset Split	13
B.2. Dataset for Training Grounding Module	14
B.3. Dataset for Training Semantic Segmentation Model	15
C Additional Ablation Study	16
C.1. Synthetic Dataset Construction.	16
C.2. Effect on the Number of Seen Categories.	16
C.3. Dataset Construction via DDIM Inverse.	16
D More Qualitative Results	18
E Limitation & Future Work	18

In this supplementary document, we start by giving more details on the architecture of our grounding module in Section A, followed by the details for generating the dataset for training it in Section B; then describe the additional ablation studies, as promised in the main text in Section C; In Section D, we present more qualitative results; Lastly, we illustrate the limitation of our method and our future work in Section E.

A. Details on the Architecture of Grounding module

We show the detailed architecture of our grounding module in Fig. 8, which consists of visual encoder, text encoder, transformer decoder and MLP in the fusion module.

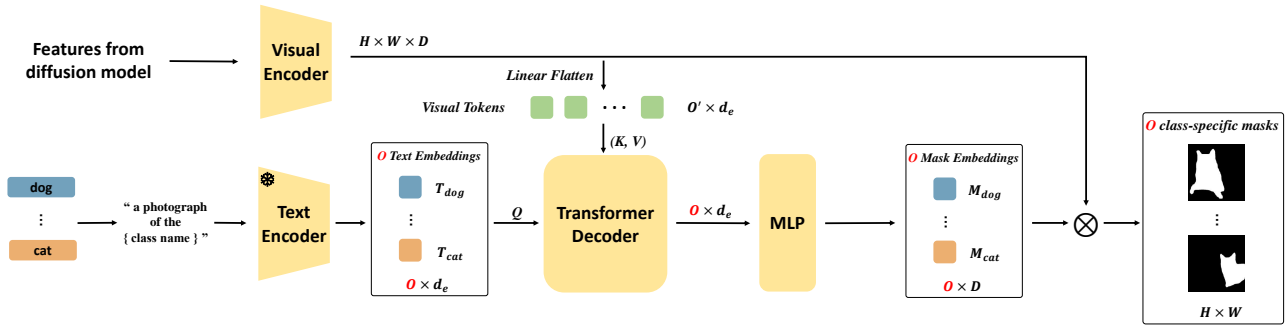


Figure 8. **Detailed architecture of our grounding module.** We first generate \mathcal{O} text embeddings by injecting the class names into a prompt template and then feeding them to a pre-trained text encoder. The visual encoder takes the features from Stable Diffusion as input and outputs fused visual features, which are then flattened to a sequence of visual tokens. Next, we feed the visual tokens into a transformer decoder as *Key* and *Value*, and feed text embeddings as *Query*. The outputs of transformer decoder are then fed into an MLP to obtain \mathcal{O} mask embeddings. Mask embeddings are dot producted with the output features of visual encoder to generate \mathcal{O} class-specific binary masks.

Visual Encoder. The input $\{f^1, \dots, f^n\}$ are extracted from Stable Diffusion [27], and the visual encoder aims to upsample and fuse the visual feature, and output the visual feature map, $\hat{\mathcal{F}} = \Phi_{v\text{-enc}}(\{f^1, \dots, f^n\})$, $\hat{\mathcal{F}} \in \mathbb{R}^{H \times W \times D}$ (here we use $H = W = 512$, and $D = 240$). Note that, the resolution of the fused visual feature is the same as the resolution of the generated image, and the segmentation masks.

Text Encoder. We adopt the pre-trained text encoder from CLIP [25], which is also used in Stable Diffusion [27]. It takes text prompt y as input and outputs the corresponding text embedding: $\mathcal{E}_{\text{object}} = \Phi_{t\text{-enc}}(y)$, $\mathcal{E}_{\text{object}} \in \mathbb{R}^{\mathcal{O} \times d_{\text{text}}}$, where \mathcal{O} is the total number of objects of interest and $d_{\text{text}} = 768$.

Transformer Decoder in Fusion Module. Similar to the operation in standard ViT architecture [8], we convert the visual features $\hat{\mathcal{F}} \in \mathbb{R}^{H \times W \times D}$ into visual tokens $\hat{\mathcal{F}}_{\text{flatten}} \in \mathbb{R}^{\mathcal{O}' \times d_{\text{visual}}}$, where $\mathcal{O}' = \frac{HW}{p^2} = 16384$ is the number of tokens, p refers to the patch size and $d_{\text{visual}} = p^2 \times D = 3840$. Then the visual tokens and text embeddings are mapped into the same dimension $d_e = 512$ with MLPs, and passed into the transformer decoder with three layers. The text embeddings are treated as query with dimension $\mathcal{O} \times d_e$, and the visual tokens are treated as key and value with dimension $\mathcal{O}' \times d_e$. The output of transformer decoder is of the same resolution as query, with dimension $\mathcal{O} \times d_e$.

MLP in Fusion Module. At last, we use an MLP to map the output of transformer decoder into mask embeddings with dimension $\mathcal{O} \times D$, which are then dot producted with the fused visual feature ($\hat{\mathcal{F}} \in \mathbb{R}^{H \times W \times D}$) to generate class-specific binary masks ($\mathcal{O} \times H \times W$), each mask is of the same spatial resolution of the generated image.

B. Details on the Synthetic Dataset

B.1. Dataset Split

Here, to train our proposed grounding module, and properly evaluate its ability for segmenting the objects that are unseen at training time, we construct the training dataset with images of only seen categories, and the test dataset consists of both seen and unseen categories. The detail of the split on PASCAL-sim and COCO-sim, *i.e.* the split of seen categories and unseen categories, is shown in Tab. 4, where PASCAL-sim has 15 seen categories and 5 unseen categories, COCO-sim has 65 seen categories and 14 unseen categories. Note that, we ignore the category: ‘mouse’ in the COCO-sim since the diffusion model generates ‘rat’ in the image for the category: ‘mouse’, while ‘mouse’ in the vocabulary of the off-the-shelf detector means mouse as a computer accessory, thus the detector fails to detect the category ‘mouse’ in the image generated by the diffusion model.

	Categories	seen	Unseen
PASCAL-sim	Split1	aeroplane, bicycle, bird, boat, bottle, bus, cat, chair, cow, diningtable, horse, motorbike, person, pottedplant, sheep	tvmonitor, car, dog, sofa, train
	Split2	tvmonitor, car, dog, sofa, train, aeroplane, bicycle, bird, boat, bottle, bus, cat, chair, cow, diningtable	horse, motorbike, person, pottedplant, sheep
	Split3	horse, motorbike, person, pottedplant, sheep, tvmonitor, car, dog, sofa, train, aeroplane, bicycle, bird, boat, bottle	bus, cat, chair, cow, diningtable
COCO-sim	Split1	person, bicycle, car, motorbike, bus, truck, boat, traffic light, fire hydrant, stop sign, bench, bird, dog, horse, sheep, cow, elephant, zebra, giraffe, backpack, umbrella, handbag, tie, skis, sports ball, kite, baseball bat, baseball glove, skateboard, surfboard, tennis racket, bottle, wine glass, cup, knife, spoon, bowl, banana, apple, orange, broccoli, carrot, pizza, donut, cake, chair, bench, pottedplant, bed, diningtable, tvmonitor, laptop, remote, keyboard, cell phone, microwave, oven, sink, refrigerator, book, clock, vase, scissors, teddy bear, toothbrush	aeroplane, train, parking meter, cat, bear, suitcase, frisbee, snowboard, fork, sandwich, hot dog, toilet, toaster, hair drier
	Split2	aeroplane, train, parking meter, cat, bear, suitcase, frisbee, snowboard, fork, sandwich, hot dog, toilet, toaster, hair drier, person, bicycle, car, motorbike, bus, truck, boat, traffic light, fire hydrant, stop sign, bench, bird, dog, horse, sheep, cow, elephant, zebra, giraffe, backpack, umbrella, handbag, tie, skis, sports ball, kite, baseball bat, baseball glove, skateboard, surfboard, tennis racket, bottle, wine glass, cup, knife, spoon, bowl, banana, apple, orange, broccoli, carrot, pizza, donut, cake, chair, bench, pottedplant, bed, diningtable, tvmonitor	laptop, remote, keyboard, cell phone, microwave, oven, sink, refrigerator, book, clock, vase, scissors, teddy bear, toothbrush
	Split3	laptop, remote, keyboard, cell phone, microwave, oven, sink, refrigerator, book, clock, vase, scissors, teddy bear, toothbrush, aeroplane, train, parking meter, cat, bear, suitcase, frisbee, snowboard, fork, sandwich, hot dog, toilet, toaster, hair drier, person, bicycle, car, motorbike, bus, truck, boat, traffic light, fire hydrant, stop sign, bench, bird, dog, horse, sheep, cow, elephant, zebra, giraffe, backpack, umbrella, handbag, tie, skis, sports ball, kite, baseball bat, baseball glove, skateboard, surfboard, tennis racket, bottle, wine glass, cup, knife, spoon, bowl	banana, apple, orange, broccoli, carrot, pizza, donut, cake, chair, bench, pottedplant, bed, diningtable, tvmonitor

Table 4. The details on the split of categories on PASCAL-sim and COCO-sim.

B.2. Dataset for Training Grounding Module

To construct the training set, (1) we first randomly select one or two categories from the seen ones, where objects tend to co-appear in natural images, based on the annotation in PASCAL VOC [9] or COCO [20], called **co-appearing category pair**, and use the prompt template to decorate these selected categories, thus we can obtain the text prompt; (2) we pass the text prompt and randomly sampled Gaussian noise to the Stable Diffusion [27] to obtain the generated image; (3) next, we pass the generated image to the off-the-shelf detector to obtain the oracle segmentation mask; (4) finally, we can construct the triplet which consists of the generated image, oracle segmentation mask, and text prompt; (5) repeat the above procedure, we can generate infinite triplets for the training set. Algorithm 1 displays the procedure for generating the training set.

To construct the test set for evaluating the grounding module, we can use a procedure similar to the training set. The differences are: (i) we use all categories, including seen and unseen categories to construct the test set. (ii) to obtain more reliable test results, we only add the triplet to the test set when the generated image and oracle segmentation mask have high quality which is checked manually, *i.e.*, the generated image by Stable Diffusion contains the recognizable objects of selected categories, and the off-the-shelf detector successfully produces the high-quality oracle segmentation mask.

In this paper, PASCAL-sim has 20 categories and 142 co-appearing category pairs. We construct 30 triplets per category and 5 triplets per co-appearing category pair for PASCAL-sim test set. In total, PASCAL-sim test set has 1310 triplets. COCO-sim has 79 categories and 1559 co-appearing category pairs. We construct 30 triplets per category and 2 triplets per co-appearing category pair for COCO-sim test set. In total, COCO-sim test set has 5488 triplets.

Algorithm 1 Constructing the dataset for training grounding module (pseudocode in PyTorch-like style).

```
# C_seen: the list of seen categories
# img_shape: the shape of expected generated image
# exp_train_size: the expected size of training set
# n: the number of selected categories, n = 1 or 2
# co-appearing_category_pair_list: a list containing all co-appearing category pairs, where objects tend to
# co-appear in natural images, based on the annotation in PASCAL VOC or COCO

D_train = [] #initialize the training set

while (len(D_train) < exp_train_size):

    y = None #initialize the text prompt

    #randomly select n categories from seen categories
    selected_class_list = random_select(C_seen, n)

    if n = 1:
        class = selected_class_list[0]

        # decorate the selected category by a pre-defined prompt template, e.g., "a photograph of a [class name]"
        y = prompt_template(class)

    else if n = 2:
        class1, class2 = selected_class_list[0], selected_class_list[1]
        if (class1, class2) in co-appearing_category_pair_list:

            # decorate the selected categories by a pre-defined prompt template, e.g., "a photograph of a
            # [class1 name] and a [class2 name]"
            y = prompt_template(class1, class2)

    if y != None:

        #randomly sample a Gaussian noise epsilon
        epsilon=torch.randn(img_shape)

        # pass the noise and text prompt to the diffusion model to generate image I
        I = diffusion_model(epsilon, y)

        # pass the generated image to the off-the-shelf detector to obtain the oracle segmentation mask m
        m = pretrain_detector(I)

        # add the triplet (generated image, oracle segmentation mask, text prompt) to the training set
        D_train.append((I, m, y))
```

B.3. Dataset for Training Semantic Segmentation Model

As discussed in Sec. 4.2, we synthesize a semantic segmentation dataset for all 20 categories in PASCAL VOC [9]. Specifically, we first randomly select one category or two categories (co-appearing category pair), to obtain the text prompt, and then pass randomly sampled Gaussian noise and text prompt to the diffusion model to obtain the generated image, and use our proposed grounding module to get the corresponding segmentation mask. Thus, we can get the pair consisting of generated image and generated segmentation mask. Repeat the above procedure, we can obtain the synthetic semantic segmentation dataset at a large scale. Algorithm 2 displays the procedure for generating the synthetic semantic segmentation dataset.

In this paper, the synthetic semantic segmentation dataset consists of 500 images per category and 71 images per co-appearing category pair. Thus, there exist 10k images for 20 categories and 10082 images for 142 co-appearing category pairs in total.

Algorithm 2 Pseudo-code for generating the synthetic semantic segmentation dataset in a PyTorch-like style.

```
# C: the list of all categories
# img_shape: the shape of expected generated image
# exp_dataset_size: the expected size of synthesis semantic segmentation dataset
# n: the number of selected categories, n = 1 or 2
# co-appearing_category_pair_list: a list containing all co-appearing category pairs, where objects tend to
# co-appear in natural images, based on the annotation in PASCAL VOC or COCO

D_seg = [] #initialize the synthesis semantic segmentation dataset

while (len(D_seg) < exp_dataset_size):

    y = None #initialize the text prompt

    #randomly select n categories from all categories
    selected_class_list = random_select(C, n)

    if n = 1:
        class = select_class_list[0]

        # decorate the selected category by a pre-defined prompt template, e.g., "a photograph of a [class name]"
        y = prompt_template(class)

    else if n = 2:
        class1, class2 = select_class_list[0], select_class_list[1]
        if (class1, class2) in co-appearing_category_pair_list:

            # decorate the selected categories by a pre-defined prompt template, e.g., "a photograph of a
            # [class1 name] and a [class2 name]"
            y = prompt_template(class1, class2)

    if y != None:

        #randomly sample a Gaussian noise epsilon
        epsilon=torch.randn(img_shape)

        # pass the noise and text prompt to the diffusion model with grounding module to generate image I
        # and segmentaion mask m
        I, m = diffusion_model_with_grounding(epsilon, y)

        # add the pair (generated image, generated segmentation mask) to the synthesis semantic segmentation dataset
        D_seg.append((I, m))
```

C. Additional Ablation Study

C.1. Synthetic Dataset Construction.

We explore the effect of constructing different datasets for training the grounding module, by varying the number of objects in the images. As shown in Tab. 5, training on the combination of one and two object categories gives the best results overall.

Train Set # Objects	One		Two		
	Seen	Unseen	Seen	Seen +Unseen	Unseen
single	90.37	83.85	43.89	42.33	38.91
two	88.35	82.93	80.56	68.08	56.36
mixture	90.16	83.19	78.93	66.07	57.93

Table 5. **Ablation on dataset construction on PASCAL-sim.** The bolded number indicates the best result. Our model achieves the best performance when training on the combination of one and two object categories.

C.2. Effect on the Number of Seen Categories.

We ablate the number of seen categories to further explore the generalisation ability of our proposed grounding module. As shown in Tab. 6, the grounding module can generalise to unseen categories, even as few as five seen categories; when introducing more seen categories, the performance on unseen ones consistently improves, but decreases on seen ones, due to the increasing complexity on seen categories.

Train Set # Seen Categories / unseen categories	One		Two		
	Seen	Unseen	Seen	Seen +Unseen	Unseen
5 / 74	94.81	72.42	87.19	49.60	39.00
20 / 59	91.91	73.33	71.59	56.27	41.91
35 / 44	87.23	73.85	66.91	55.99	43.28
50 / 29	84.55	73.20	66.41	54.39	42.71
65 / 14	83.85	76.81	64.64	57.15	47.77

Table 6. **Ablation on the number of seen categories on COCO-sim.** The bolded number indicates the best result. Our model can generalise to unseen categories, even as few as five seen categories.

C.3. Dataset Construction via DDIM Inverse.

In addition to using the off-the-shelf detectors, we also consider constructing the training set by utilising the inverse process of diffusion to explicitly generate images close to those in the public dataset, for example, PASCAL VOC, and train the grounding module with the mask annotations available from the dataset.

Here, we describe an inverse procedure that enables to find a deterministic mapping from noise to images, given the sampling rule being non-Markovian, for example, Denoising Diffusion Implicit Model (DDIM) [32] with the reverse process variance to be 0. In DALL-E 2 [26], such inversion has been used to determine the noise that produces a specific image. In our considered Stable Diffusion, the image is first mapped to a latent vector z^0 by the pre-trained variational autoencoder (VAE), at each step of DDIM inversion, z^{t+1} is obtained from z^t and the predicted noise term of UNet, that takes z^t and text prompt y as input, ending up with an inverted noise z^T eventually. In this paper, we exploit such DDIM inversion to train our grounding module with the dataset constructed from real image and segmentation masks.

In particular, the first option enables to directly inherit the segmentation mask from the public dataset, and the text prompt can be manually constructed by inserting class labels into the prompt template, for example, if the segmentation mask contains ‘dog’ and ‘cat’, the text prompt can be ‘a photograph of a dog and cat’. Besides, the visual feature can be obtained by extracting the feature from the UNet of Stable Diffusion when $t = 1$ at the inversion process.

Constructed Dataset v.s. Real Dataset. We explore the difference between training on constructed dataset and real dataset (PASCAL VOC) from two perspectives. *First*, we compare their performance on PASCAL-sim dataset for grounded generation in Tab. 7 (left). Though we successfully train our grounding module on real dataset, the domain gap limits its

Dataset Type	PASCAL-sim					PASCAL-test	
	One		Two			Seen	Unseen
	Seen	Unseen	Seen	Seen+Unseen	Unseen		
real	75.67	61.26	64.08	49.23	45.14	75.19	34.80
sim(10k)	88.77	70.04	73.07	57.08	46.59	61.75	48.42
sim(40k)	90.16	83.19	78.93	66.07	57.93	64.44	53.86
sim+real	89.57	76.23	78.12	62.24	55.30	73.32	57.14

Table 7. **Ablation on the training dataset.** The bold numbers indicate the best results. Specifically, 'sim' and 'real' denote the constructed dataset and real dataset (PASCAL-VOC), respectively.

performance on grounded generation task. Considering PASCAL VOC only contains about 10k images, we adjust the constructed dataset to the same magnitude and get better results. Additionally, because of the good scalability of the constructed dataset, the performance will be better as the number of images increases. *Second*, we evaluate the grounding module on PASCAL VOC test dataset by DDIM inversion as shown in Tab. 7 (right). Note that, under this circumstance, our model approximates a discriminative model. On seen categories of PASCAL VOC test set, the module trained on real dataset achieves the best result, while the module trained on constructed dataset gains an advantage on unseen categories. Besides, we also try to train our module on both constructed dataset and real dataset, which results in great improvement on PASCAL VOC test dataset but no advantage on PASCAL-sim, while the latter is our main task. Therefore, we finally choose the module training on constructed dataset as our main model.

D. More Qualitative Results

We provide more qualitative results in Fig. 9, Fig. 10, Fig. 11, and Fig. 12. Note that the images are generated from Stable Diffusion [27], and the corresponding masks are inferred from our proposed grounding module. Specifically, the generated images and their corresponding segmentation masks in Fig. 9 and Fig. 10, including common objects, *e.g.*, shark, turtle, and more unusual objects, *e.g.*, Ultraman, pterosaur, Chinese dragon, unicorn and dinosaur, shows the strong generalisability of the grounding module. In Fig. 11, we show more examples from our synthetic semantic segmentation dataset. In Fig. 12, we compare the model trained on our synthesized datasets with other ZS3 methods on PASCAL VOC dataset [9]. We can observe that the MaskFormer [4] trained on our synthetic semantic segmentation dataset can obtain accurate segmentation on both seen and unseen categories, showing that the guided text-to-image diffusion model can be used to expand the vocabulary of pre-trained detector.

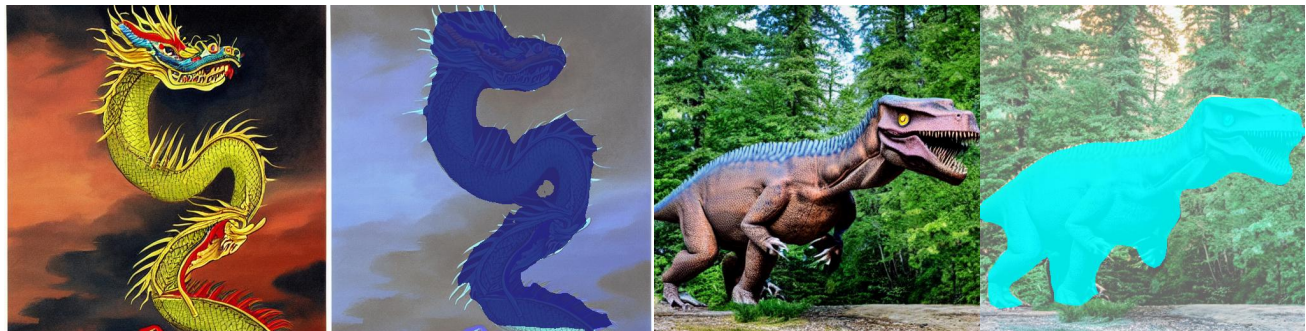
E. Limitation & Future Work

In this paper, we have demonstrated the possibility for aligning the visual and language representation of a text-to-image diffusion model, and augment it with the ability of grounding visual objects along with generation. However, we also realise there exists certain limitation in this work, *first*, we only consider to ground the nouns that indicate visual entities, it would be interesting to ground the human-object, object-object interactions, or even verbs in the future, *second*, we are inserting the grounding module to a pre-trained text-to-image generative model, it would be interesting to co-train the two components, potentially enabling to generate images with higher quality and explainability.



a photograph of a superman next to a tree

a painting of a unicorn on the snow land



a photograph of a Chinese dragon in the sky

a photograph of a dinosaur in the woods



a painting of a highly detailed wizard

a photograph of a crane in the lake



a photograph of a highly detailed Mickey

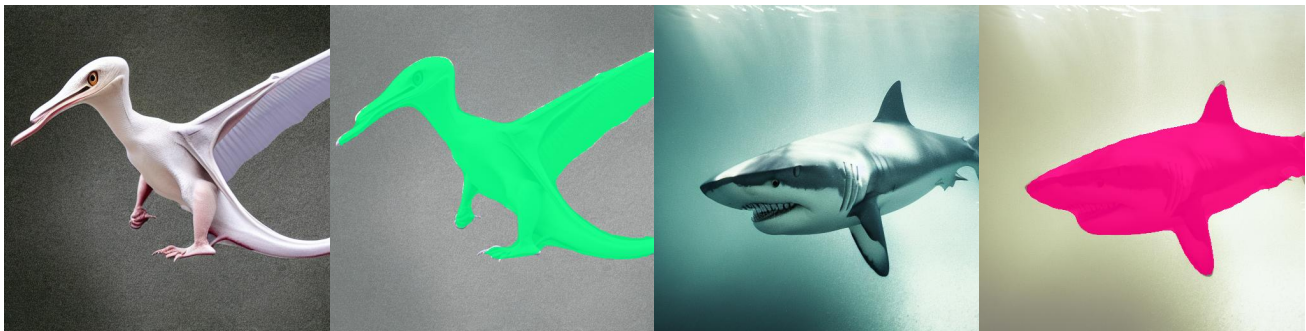
a photograph of a devilfish in the sea

Figure 9. Results of grounded generation. The segmentation mask refers to the grounding results for the object underlined.



a photograph of a launched rocket

a painting of a highly detailed Ultraman



a photograph of a white pterosaur

a photograph of a shark in the sea



a painting of a smilodon on the grass

a photograph of a whale leaping out of the sea



a photograph of a turtle crawling in the sand

a photograph of a statue of Zeus

Figure 10. **Results of grounded generation.** The segmentation mask refers to the grounding results for the object underlined.



Figure 11. Examples from our synthetic semantic segmentation dataset.

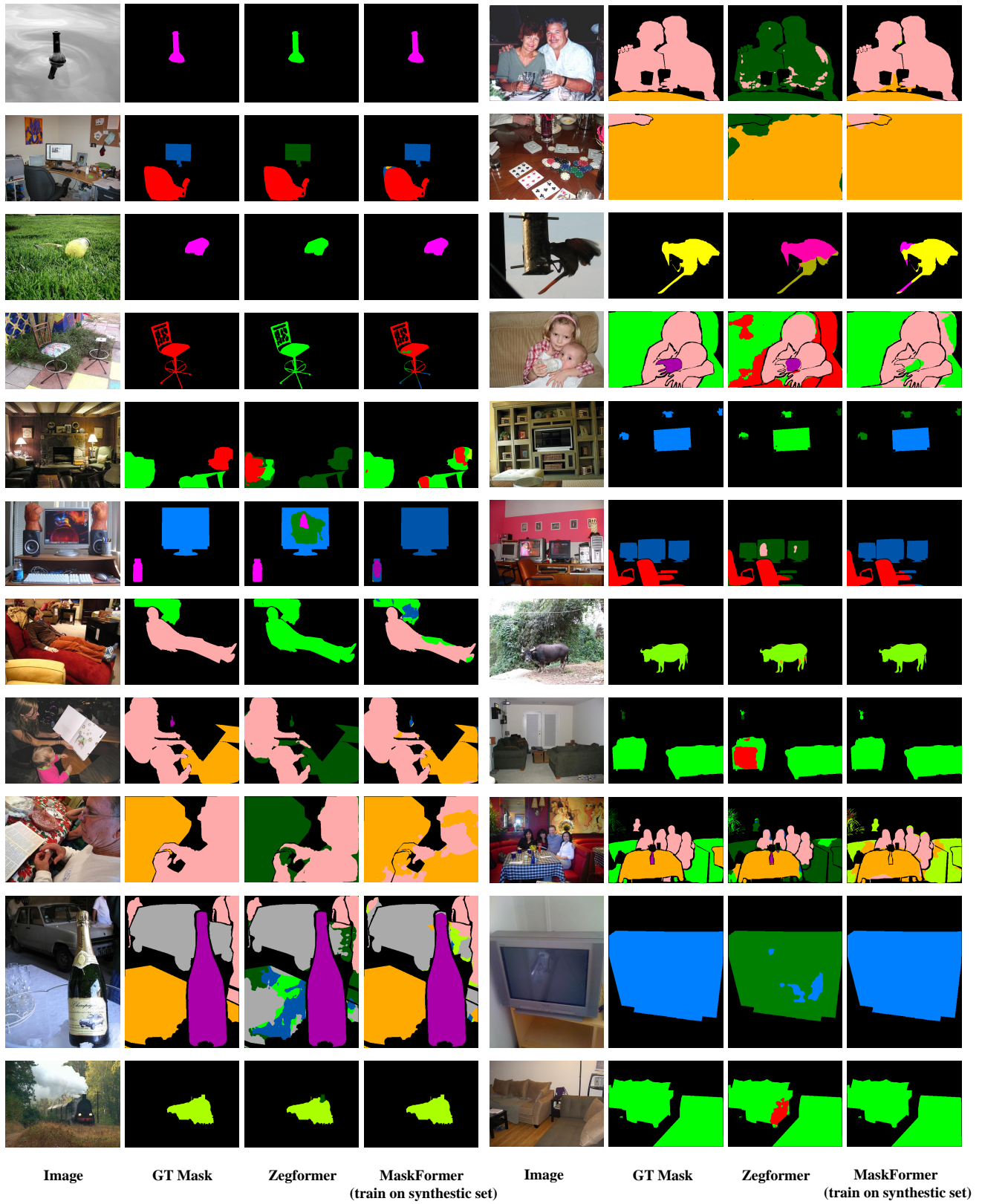


Figure 12. More visualization of zero-shot segmentation results on Pascal VOC.